ESC European Society of Cardiology

European Heart Journal - Imaging Methods and Practice (2025) **3**, qyaf007
https://doi.org/10.1093/ehjimp/qyaf007

ORIGINAL ARTICLE

Noninvasive assessment of myocardial perfusion using ultrafast ultrasound: clinical study for congenital heart disease

Minh B. Nguyen [1,2,†], Naiyuan Zhang [1,†], Luc L. Mertens [1], David Barron [3], Osami Honjo [3], Maelys Venet [1,4], Jerome Baranger [1,‡], and Olivier Villemain [1,4,5,*‡]

[1]Division of Cardiology, Department of Pediatrics, The Hospital for Sick Children, University of Toronto, 555 University Avenue, Toronto, Ontario, Canada, ON M5G 1X8
[2]Section of Pediatric Cardiology, Texas Children's Hospital, Baylor College of Medicine, Houston, TX, USA
[3]Department of Surgery, Division of Cardiovascular Surgery, The Hospital for Sick Children, University of Toronto, Toronto, Ontario, Canada
[4]Department of Pediatric and Adult Congenital Cardiology, Bordeaux University Hospital (CHU), Pessac, France, Ave Magellan, 33600 Pessac, France
[5]Electrophysiology and Heart Modeling Institute, Institut Hospital-Universitaire Liryc, Fondation Bordeaux Université, Bordeaux, France, Av. du Haut Lévêque, 33600 Pessac, France

Received 19 August 2024; accepted after revision 30 October 2024; online publish-ahead-of-print 16 January 2025

Abstract

Aims

Myocardial perfusion impacts cardiac function following surgical repair of critical congenital heart disease (CCHD). Temporal variation assessment of myocardial blood volume throughout the cardiac cycle can be a surrogate for perfusion. Ultrafast power Doppler (UPD) is an ultrasound imaging technique capable of noninvasively quantifying myocardial blood volume changes. The objective of this study is to demonstrate the feasibility of perioperative transthoracic UPD assessment and to determine if UPD reflects physiologic changes in myocardial perfusion.

Methods and results

Five neonatal transposition of the great arteries (TGA) undergoing arterial switch operation (ASO), five hypoplastic left heart syndrome (HLHS) undergoing Stage 1 palliation (S1P), and five age/weight-matched controls were prospectively recruited. Transthoracic UPD acquisitions were performed before/after operations. Segmental perfusion in right/left ventricles (RV/LV) was assessed. The controls' myocardial perfusion patterns are visually similar to published human references for both ventricles. Systolic/diastolic myocardial perfusion differences were modified by ASO in the RV ($P = 0.03$) but not for LV ($P = 0.99$). For HLHS patients, no difference after S1P was observed in either the RV ($P = 0.16$) nor the LV ($P = 0.51$).

Conclusion

For TGA patients, the perfusion profile of the myocardium seems to be directly influenced by the intracavitary pressure (directly driving coronary perfusion pressure), namely if it was the systemic or sub-pulmonary ventricle. Our data suggests that UPD could noninvasively quantify myocardial perfusion variation. Myocardial perfusion patterns change in CCHD according to their haemodynamic and surgical status. Correlation with clinical outcomes requires further study.

* Corresponding author. E-mail: olivier.villemain@chu-bordeaux.fr; Twitter: @Villemain_Team
† Co-first authors.
‡ Co-last authors.

Graphical Abstract

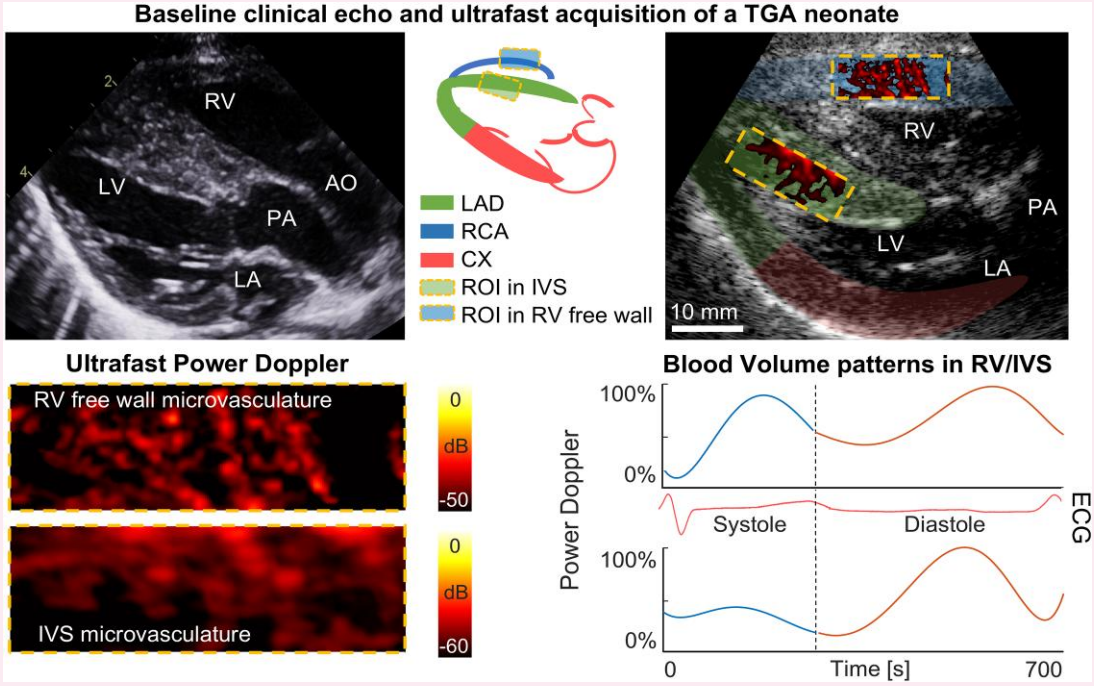

Visualizing moving blood volumes using ultrafast power Doppler. An ultrafast ultrasound scanner was used to acquire transthoracic sequences in a pre-operative TGA patient. Power Doppler signals are extracted from a region of interest, and the mean power Doppler signal is plotted over time. TGA, transposition of the great arteries; RV, right ventricle; IVS, interventricular septum.

Keywords myocardial perfusion • critical congenital heart disease • ultrafast ultrasound

Introduction

Myocardial perfusion is a key mediator of morbidity and mortality in cardiac surgery, especially with coronary artery manipulation.[1,2] Adequate coronary arterial function impacts outcomes, especially in neonates with transposition of the great arteries (TGA) undergoing an arterial switch operation (ASO), as adequacy of coronary translocation is linked to adverse events in TGA.[3] Additionally, inadequate myocardial perfusion is associated with poor outcomes in children with hypoplastic left heart syndrome (HLHS) undergoing stage 1 palliation (S1P).[4,5]

Current diagnostic modalities that assess myocardial perfusion often do so as a perfusion rate averaged over several heartbeats (i.e. millilitres per gram per minute).[6] However, temporal variations of perfusion within a cardiac cycle are sensitive to physiologic changes both upstream and downstream of the coronary vasculature. For example, coronary perfusion pressure (i.e. the difference between ventricular and arterial pressure) produces markedly different temporal perfusion patterns in a normal right vs. left ventricle.[7] Furthermore, changes in autoregulation (e.g. vagal or adrenergic stimulation) can also significantly impact perfusion patterns.[8] However, current noninvasive diagnostic modalities do not present temporal fluctuations in coronary perfusion patterns within one cardiac cycle, often due to issues in spatiotemporal resolution.[6]

Ultrafast ultrasound imaging permits this spatiotemporal detection with high sensitivity. Its ability to detect myocardial perfusion has been validated against perfusion rates with epicardial coronary flow metre techniques in animal studies.[9–11] Ultrafast power Doppler (UPD) assessment could also be used to assess temporal variations in blood volume patterns. Blood volume assessment using power Doppler (PD), which is proportional to the density of red blood cells, has been shown to strongly associate with perfusion, the rate of moving blood through an organ, in conventional ultrasound studies.[12–14]

The aims of this study are (i) to demonstrate the feasibility of peri-operative transthoracic UPD assessment and (ii) to determine if UPD can describe the physiologic changes in coronary perfusion before and after surgery.

Methods

Study design

This was a single centre, prospective cohort study. We prospectively enrolled neonates diagnosed with TGA with intact ventricular septum undergoing ASO, those with HLHS undergoing S1P, and healthy volunteers (neonates with normal cardiac structure and function) at the Hospital for Sick Children in Toronto, Ontario, Canada. Ultrafast transthoracic echocardiograms were performed during the first week of life and, if the patient was part of a congenital heart disease cohort, another acquisition was performed at least 7 days after cardiac surgery (*Figure 1A* and *B*). Children were followed for up to thirty days after surgery and assessed for major complications, including death, reintervention (surgical or catheter-based), and cardiac-related readmissions. The pre-operative clinical echocardiogram and discharge echocardiogram were assessed. The study was approved by the local review ethics board (REB number: 1000070089), and all parents gave written informed consent.

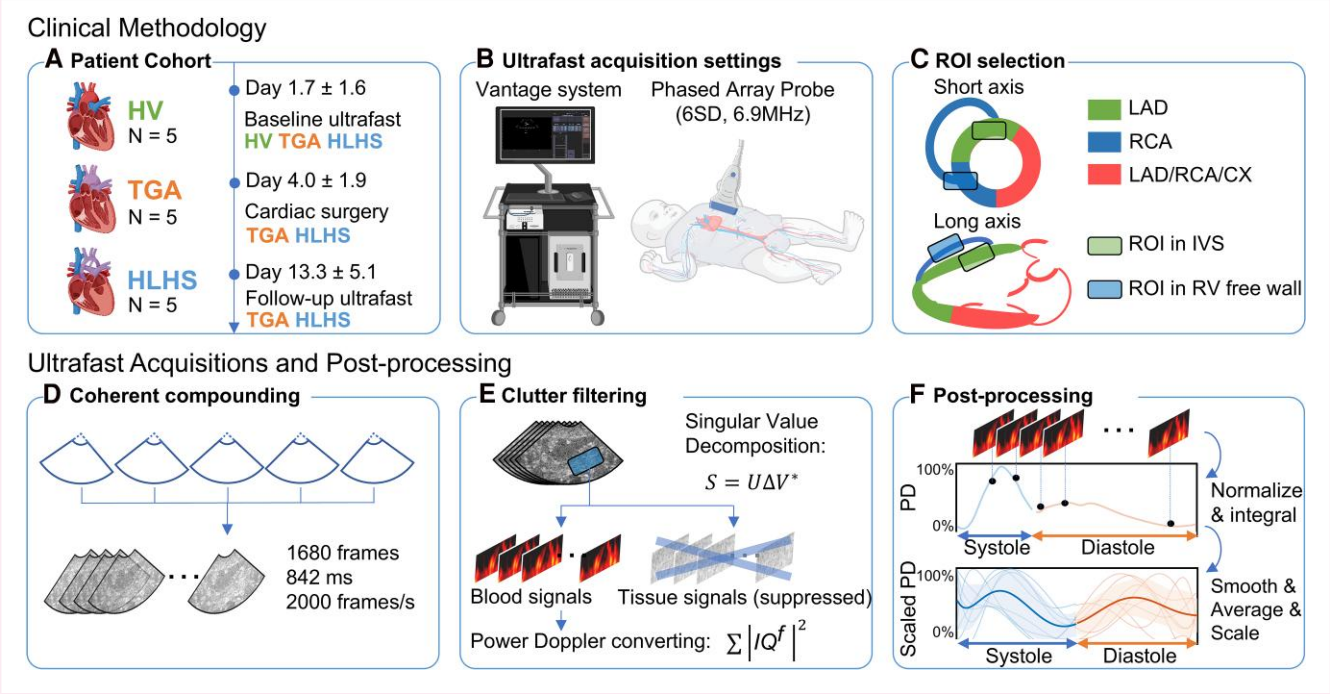

Figure 1 The acquisition workflow for ultrafast PD myocardial perfusion approximation. (*A*) HV, TGA with intact ventricular septum, and HLHS were recruited. (*B*) An ultrafast ultrasound-enabled research scanner was used in all acquisitions. (*C*) Three acquisitions were acquired in the short and long-axis views at the RV free wall and interventricular septum. (*D*) Ultrafast acquisitions were taken at 2000 frames per second, with coherent compounding of 5 diverging waves (top row), covering a sector of 60°, with an imaging depth of 60 mm. (*E*) After tissue signals were suppressed, ultrafast ultrasound PD signals were extracted to quantify blood volumes of the coronary microvasculature. (*F*) PD signals were plotted over time and, for visualization purposes, scaled by peak PD throughout the cardiac cycle and by maximal time duration. HV, healthy volunteer; TGA, transposition of the great arteries; HLHS, hypoplastic left heart syndrome; LAD, left anterior descending artery; RCA, right coronary artery; Cx, circumflex; IVS, interventricular septum; RV, right ventricle; PD, power Doppler.

General experimental approach

Conventional PD has been shown to strongly associate with perfusion rate.[14] In vitro and *in vivo* studies have demonstrated that UPD could estimate blood volumes reliably.[15] We have therefore elected to quantify blood volume patterns within a myocardial segment throughout the cardiac cycle using UPD. We compared our blood volume pattern assessments in healthy volunteers against reference perfusion patterns derived from epicardial coronary flow probe assessment, a gold standard perfusion diagnostic technique with high temporal resolution.[7] We then compared our perfusion patterns amongst our three cohorts: healthy volunteers, TGA patients, and HLHS patients. Finally, we explored if our perfusion patterns were coherent against the gold standard reference patterns and physiologic changes induced by cardiac surgery.

Image acquisition and reconstruction

The ultrasound methodology has been described in previous works by our team.[16] An overview of the acquisition and reconstruction process is illustrated in Supplementary data online, *Figure S1*. Additionally, the process is presented within the context of the full study in *Figure 1*. Briefly, ultrafast ultrasound imaging was performed on each patient using a programmable ultrafast ultrasound system (Vantage 256, Verasonics Inc., Kirkland, WA, USA) with a phase array probe (GE 6SD, 6.9 MHz, GE Healthcare, USA) (*Figure 1D*). The image depth was 60 mm and the sector width was 60°. We used coherent compounding of five diverging waves whose virtual sources were equally spread along the transducer aperture as in Correia *et al.*[17] Each acquisition was triggered by the R wave while electrocardiogram was recorded and lasted 842 ms with 1680 images at a framerate of 2000 Hz, secondly such that at least one full cardiac cycle was imaged.

Transthoracic echocardiography was performed by a trained cardiologist (Minh Bao Nguyen). Three parasternal short and three parasternal long-axis acquisitions were obtained for each patient. A conventional line-by-line B-mode view was utilized to allow the operator to identify the correct position and location in real time. A high framerate acquisition is then triggered by the operator. After each acquisition, image reconstruction was automatically performed on the cart to allow for a 2D/B-mode image to be reviewable to the operator if necessary. The typical exam duration was 5 min with about 30 s needed for probe positioning using real-time B-mode imaging, 2 s for data acquisition and storage, and 15 s for pre-processing steps (image reconstruction). The best clip was chosen for PD quantification by assessing the 2D image for visual quality and correct alignment as per paediatric transthoracic echocardiography guidelines.[18]

A region of interest (ROI) was placed on the anterior right ventricular free wall (RV perfusion) and the basal anteroseptal interventricular septum (LV perfusion), see *Figure 1C*. The depth of the ROIs was adjusted to match the unique anatomy of each patient, with a typical average depth of 8–18 mm for the RV ROI and 20–30 mm for the LV ROI. For a given patient, the size of the RV and LV ROIs were identical but varied across patients depending on their anatomy, ranging typically from 20 to 30 mm^2.

We applied singular value decomposition as an adaptive clutter filter with a sliding window approach that we previously developed.[15] In brief, we divided the 842-ms-long acquisition into smaller temporal sliding windows with a 50% overlap. The duration of each sliding window was adapted such that the tissue motion during this period was kept below one wavelength (250 μm). The underlying idea is that longer windows ensure higher efficiency of the clutter filtering, provided that the tissue can be considered stationary during said window. Our approach optimizes the size of the sliding window along the cardiac cycle in such a manner that windows are shorter (typically 25 ms) in systole when the heart walls motion is high,

and longer in late diastole (typically 50 ms) when the walls are almost steady. To extract the blood signal, the tissue signal was removed using an adaptive singular value decomposition filter on each sliding window. The blood signal (i.e. the filtered complex IQ data) was averaged over overlapping windows and converted into PD by simply computing the square of its amplitude (*Figure 1E*). As a quantitative metric, we did not perform the conventional conversion of PD values to decibels (i.e. a technique that scales pixel intensity by the maximum pixel value in each frame and log-compressed). Instead, we used the raw PD value (i.e. the unadjusted blood signal intensity of a given pixel), which is proportional to the local concentration of red blood cells.[19]

PD visualization and quantification

We were interested in quantifying temporal changes in blood volume patterns throughout the cardiac cycle. To do so, for a given time point, we averaged the PD value of all pixels inside each ROI (*Figure 1F*), yielding a single averaged PD time trace for each region.

PD is sensitive to both technical settings (e.g. depth of the ROI, elevation width) and clinical parameters (e.g. haematocrit) making it difficult to be compared across events and between patients.[12,14,19] To account for this, we scaled our PD values to the maximum PD value throughout the cardiac cycle since haematocrit and the depth of the myocardium are unlikely to change significantly within that time period (*Figure 1F*). Calculating the time integral of the scaled PD (power Doppler integral, PDI) values in systole and in diastole allows for a comparison of relative blood volume changes within a single cardiac cycle. This permits the comparison of systolic and diastolic blood volume in different patient groups and physiologies (e.g. before and after surgery). As each patient had different durations of systole and diastole before and after surgery, the PD trace during each phase had a varying number of samples. To allow comparison across patients, we therefore resampled each PD trace using cubic interpolation so that both systolic and diastolic signals had exactly 420 temporal samples, corresponding to 210 ms (see Supplementary data online, *Figure S1*). It must be emphasized that the quantitative PDI values were computed before the temporal scaling of systole and diastole and therefore were unaffected by this resampling operation. The latter was performed to allow visual comparisons between different perfusion patterns. We then fitted a generalized additive model to the median PD curve (across patients) as a function of time to provide a visual summary of temporal changes throughout the cardiac cycle. We did this for each operative status and patient diagnosis (*Figure 1F*).

Statistical analysis

For univariate analysis, data for continuous variables were presented as mean and standard deviation or as median and interquartile range as appropriate. Categorical variables were presented as frequencies and percentages. PDI was compared between systole and diastole across patients and operative states. To understand relative differences in PDI within a cardiac cycle, we converted PDI into percentages (e.g. systolic PDI percentage = systolic PDI/sum of systolic and diastolic PDI). The mean PDI difference in diastole compared with systole of each group was then obtained by calculating the mean diastolic PDI percentage minus the mean systolic PDI percentage and a two-sample Student's *t*-test was applied to these groups. To compare the relative difference in blood volumes within cardiac cycles between other groups, we performed a *t*-test on the mean PDI difference in diastole compared with systole between each group. For example, to compare relative changes of blood volumes within a cardiac cycle of a pre-operative TGA RV vs. a post-operative TGA RV, we assessed the mean PDI difference in diastole compared with systole of the pre- and post-operative RV. Statistical significance was assigned at $P < 0.05$. Image acquisition, PD extraction, and statistical analyses were performed using MATLAB (Release 2019a, The MathWorks, Inc., Natick, MA, United States).

Results

We recruited five neonates with TGA, five neonates with HLHS, and five healthy volunteers. Other than their diagnosis and timing of surgery, there was no significant difference between the three groups in terms of demographics (including gestational age, sex, and weight) (*Table 1*). The healthy volunteer postnatal age at the time of study mean is 14 days ± 11. There is no significant difference between groups' ages by independent *t*-test (*P*-value >0.05). Of the HLHS patients, two had mitral atresia with aortic atresia, and three had mitral stenosis with aortic atresia. Four TGA patients underwent a pre-surgical balloon atrial septostomy (*Table 1*). All five TGA patients had a moderate or large patent ductus arteriosus.

Intraoperative and post-operative characteristics

With respect to operative characteristics, one TGA had aortic arch hypoplasia requiring ASO and arch reconstruction while the remaining TGA patients underwent ASO. All HLHS patients underwent the Norwood Sano modification.[4] Bypass and cross-clamp times were similar across the TGA and HLHS groups (*Table 2*). TGA patients were cooled to 34°C without deep cardiac hypothermic arrest (DCHA), while HLHS patients were cooled to 18°C and DCHA was implemented for the aortic arch repair.

With respect to outcomes, most patients had no complications in the first 30 days after surgery. One TGA patient with a CHD7 mutation associated with CHARGE syndrome was terminally extubated due to poor respiratory drive, which was thought to be related to an associated neuromuscular disorder discovered post-operatively. From a cardiac standpoint, they had an uncomplicated ASO with signs of normal ventricular function and cardiac output. One HLHS patient had persistent cyanosis after S1P related to bilateral pulmonary artery stenosis requiring catheter intervention. This patient was admitted for more than 30 days post-operatively for feeding rehabilitation. On the discharge echocardiogram, all surviving patients (9/10) had good ventricular systolic function except for one TGA patient who had mildly reduced RV systolic function.

Temporal patterns for myocardial perfusion

Each individual patient's temporal PD pattern is presented in Supplementary data online, *Figure S2*. The patient's patterns are then summarized by diagnosis and presented in *Figures 2–4*.

- Healthy volunteers ($n = 5$)

In the RV, the mean PDI difference in diastole compared with systole was −11% (95 confidence interval, CI: −19–2.5, $P = 0.14$). In the LV, the difference was 30% (95 CI: 22–38, $P = 0.001$). On visual comparison, the right ventricular blood volume pattern appeared similar to the reference standard coronary perfusion pattern with a slightly higher peak in systole than diastole (*Figure 2*). Meanwhile, the left ventricular blood volume pattern had an early peak in diastole with a relatively suppressed systolic peak similar to the reference standard (*Figure 2*).

- TGA ($n = 5$)

Before ASO, the RV perfusion in diastole was statistically higher than the systolic perfusion (mean PDI difference in diastole compared with systole = 47%, 95 CI 35–58, $P = 0.003$) (*Figure 3*). Visually, this appeared similar to the blood volume patterns of a healthy volunteer's LV. After the ASO, where the RV is no longer pressurized by systemic afterload, the RV mean PDI difference in diastole compared with systole was no longer statistically significantly different (13%, 95 CI 15–25, $P = 0.43$). Visually, there was a slightly higher peak in systole relative to diastole, which is similar to a healthy volunteer RV perfusion (*Figure 3*). The LV perfusion, which was pressurized via a patent ductus arteriosus, had a peak in diastole with a blunted curve in systole, and this pattern did not change post-operatively (*Figure 3*).

To quantify the impact of the ASO on coronary perfusion, we performed a *t*-test on the mean PDI difference in diastole compared with

Table 1 Demographic and diagnostic characteristics

Characteristic	TGA, *N* = 5	HLHS, *N* = 5	HV, *N* = 5	*P*
Gestational age (weeks)	38.00 (38.00, 38.25)	40.00 (38.75, 40.25)	39.00 (35.50, 41.00)	0.27
Sex				
F	3 (60%)	2 (40%)	2 (40%)	
M	2 (40%)	3 (60%)	3 (60%)	
Birth weight (kg)	3.30 (2.91, 4.02)	3.30 (2.78, 3.53)	2.83 (2.46, 3.00)	0.50
Genetic abnormality				
CHD7	1 (20%)	0 (0%)	0 (0%)	
KMT2D	0 (0%)	1 (20%)	0 (0%)	
Negative microarray	2 (40%)	4 (80%)	0 (0%)	
Unknown	2 (40%)	0	0 (0%)	
Timing of diagnosis				
Prenatal	2 (40%)	5 (100%)		
Postnatal	3 (60%)	0 (0%)		
Age at surgery (days)	7.00 (5.50, 7.25)	3.00 (3.00, 4.25)		0.02
Preop Echo function				
Good biventricular systolic function	4 (80%)	0 (0%)		
Good right ventricular systolic function	0 (0%)	5 (100%)		
Mildly reduced right ventricular function	1 (20%)	0 (0%)		
PDA size				
Large	4 (80%)	5 (100%)		
Small	1 (20%)	0 (0%)		
PGE given Preop	2 (40%)	5 (100%)		
Coronary anatomy				
1LC × 2R	5 (100%)	5 (100%)		
Balloon atrial septostomy	4 (80%)	0 (0%)		
HLHS morphology				
MA/AA	0 (NA%)	2 (40%)		
MS/AS	0 (NA%)	3 (60%)		

Median (IQR); *n* (%); *P*-values derived from Kruskal–Wallis or Friedman tests.
Preop, pre-operative; PDA, patent ductus arteriosus; PGE, prostaglandin; 1LC × 2R, left anterior descending and circumflex off the left facing cusp, right coronary off the right facing cusp; HLHS, hypoplastic left heart syndrome; MA, mitral atresia; AA, aortic atresia; MS, mitral stenosis; AS, aortic stenosis; HV, healthy volunteer.

systole before and after ASO. In the RV, it was 33% (95 CI: 9–57%, $P = 0.03$), suggesting there was a change in perfusion patterns associated with the operation. In the LV it was −0.1% (95 CI: −12 to −13%, $P = 0.99$), suggesting no difference with respect to the operation.

- HLHS ($n = 5$)

Before S1P, the RV perfusion was statistically identical between systole and diastole (mean PDI difference in diastole compared with systole = −19%, 95 CI −37 to −2, $P = 0.11$) (*Figure 4*). Visually, this appeared similar to the blood volume patterns of a healthy volunteer's RV. After S1P, the RV perfusion continued to be almost identical between diastole and systole (7%, 95 CI −8 to 22, $P = 0.77$). Visually, there was a slightly higher peak in systole relative to diastole, which is similar to a healthy volunteer RV (*Figure 4*). The LV perfusion had a slight peak in systole relative to diastole, and this pattern did not change postoperatively (*Figure 4*).

Similarly to the TGA group, we performed a *t*-test on the mean PDI difference in diastole compared with systole before and after S1P. In the RV, it was 26% (95 CI: −0.59 to 7%, $P = 0.16$). In the LV it was 0.13% (95 CI: −17 to −42%, $P = 0.51$). Both tests suggest no difference in either ventricle with respect to the operation.

Discussion

In this study, we aim to evaluate the feasibility of myocardial blood volume pattern assessment using UPD. We first found that blood volume patterns as detected by ultrasound are similar to normal reference coronary perfusion patterns found in the literature. Additionally, we found that myocardial blood volume patterns change significantly after ASO while they are not affected by the first stage Norwood procedure.

We have previously demonstrated that UPD detected changes in myocardial blood volume patterns before and after cardiac surgery using epicardial ultrasound acquisitions of the left ventricle.[20] This current study builds directly on our prior work by testing UPD's feasibility with transthoracic ultrasound. This is innovative both technically and clinically. From a technical standpoint, several enhancements were necessary to use UPD on transthoracic ultrasound acquisitions, including transitioning from a high-frequency linear probe to a phased array probe and accommodating for reduction in spatial resolution due to the additional heterogenous tissue between the chest wall and the heart. Clinically, expanding UPD's use to transthoracic probes greatly expands its use case beyond the operating room in situations where perfusion assessment is much needed, such as the clinic, the intensive care unit, and the catheterization laboratory. Additionally, we could

Table 2 Operative characteristics

Characteristic	TGA, *N* = 5	HLHS, *N* = 5	*P*
Pre-operative ultrasound age (days)	2.00 (1.75, 4.5)	1.00 (1.00, 2.25)	0.19
Age at surgery (days)	7.00 (5.50, 7.25)	3.00 (3.00, 4.25)	0.02
Post-operative ultrasound age (days)	12.00 (10.75, 16.00)	16.00 (13.50, 46.25)	0.14
Surgery type			
ASO	4 (80%)	0 (0%)	
Nor/Sano	0 (0%)	5 (100%)	
ASO Arch	1 (20%)	0 (0%)	
Cardioplegia type			
Del Nido	4 (80%)	3 (60%)	
CPB (m)	135 (111.50, 160.50)	139 (132.25, 151.75)	0.60
Cross-clamp (m)	86.00 (77.75, 96.25)	87 (77.25, 97.50)	0.91
DHCA (m)		20.00 (16.75, 21.00)	
Not applicable	5	0	
SACP (m)		41.00 (36.75, 49.25)	
Not applicable	5	0	
Minimal temp (°C)		18 (18, 18)	
Not applicable	5	0	

Median (IQR); *n* (%); *P*-values derived from Kruskal–Wallis tests.
ASO, arterial switch pperation; Nor/Sano, Norwood Sano; Arch, arch reconstruction; CPB, cardiopulmonary bypass, DHCA, deep hypothermic circulatory arrest; SACP, selective antegrade cerebral perfusion.

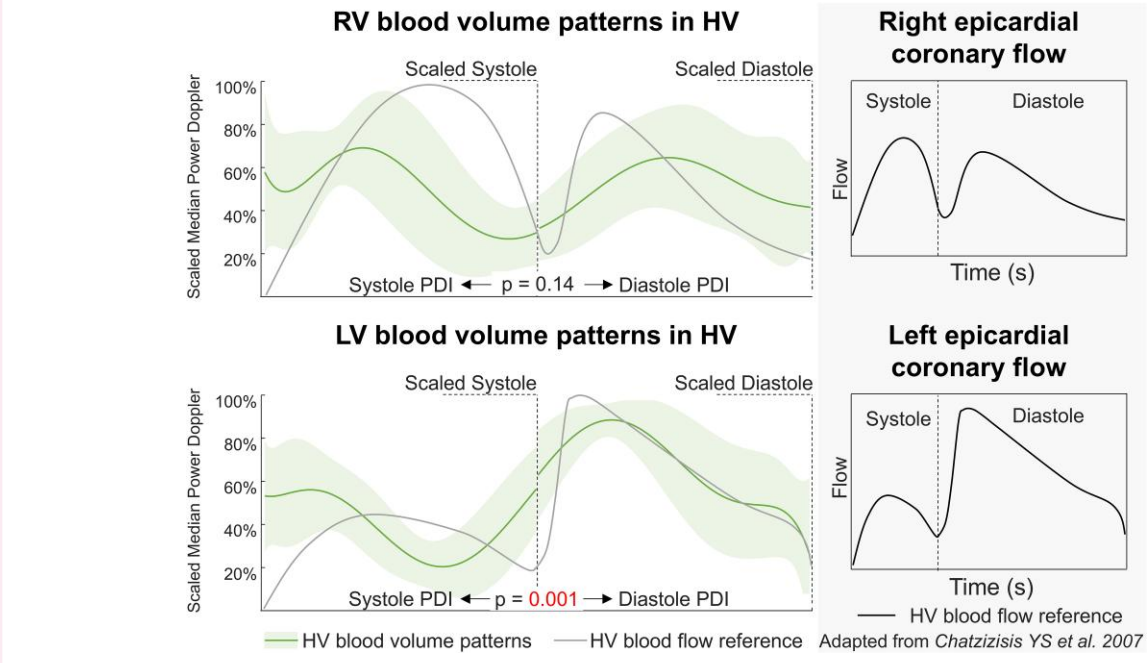

Figure 2 Temporal blood volume patterns of healthy volunteers. The right ventricular blood volume peaks slightly in systole compared with diastole. Meanwhile, the left ventricular blood volume pattern has a tall peak in diastole relative to systole. When compared with epicardial coronary perfusion data, the temporal patterns appear similar. The reference coronary perfusion pattern was scaled and superimposed onto the healthy volunteer blood volumes to assist with comparison. *P*-value derived from *t*-test comparing the difference of percentage of the integral of the PD values of systole compared with diastole. Adapted from Chatzizisis *et al.*[7]

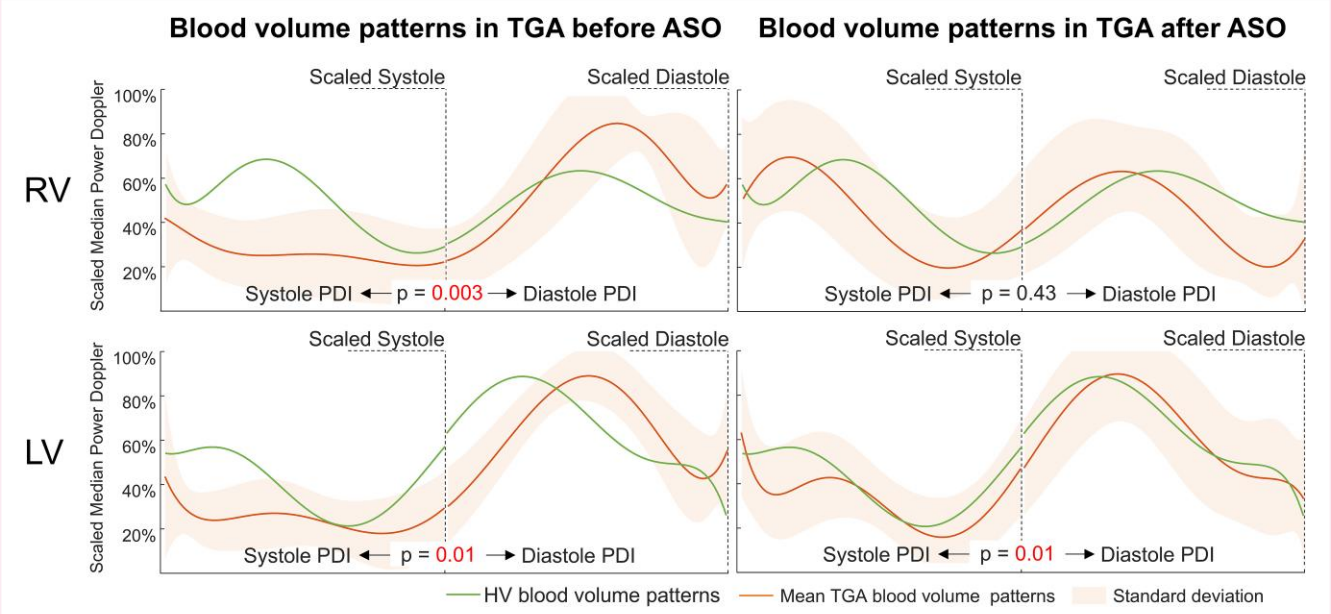

Figure 3 Temporal blood volume patterns in transposition of the great arteries. The mean blood volume patterns of TGA patients are presented. The blood volume patterns of HV are superimposed. Of note, all TGA patients pre-operatively had a patent ductus arteriosus, thus exposing the LV to systemic pressures. *P*-value derived from *t*-test comparing the difference of percentage of the integral of the PD signals of systole compared with diastole.

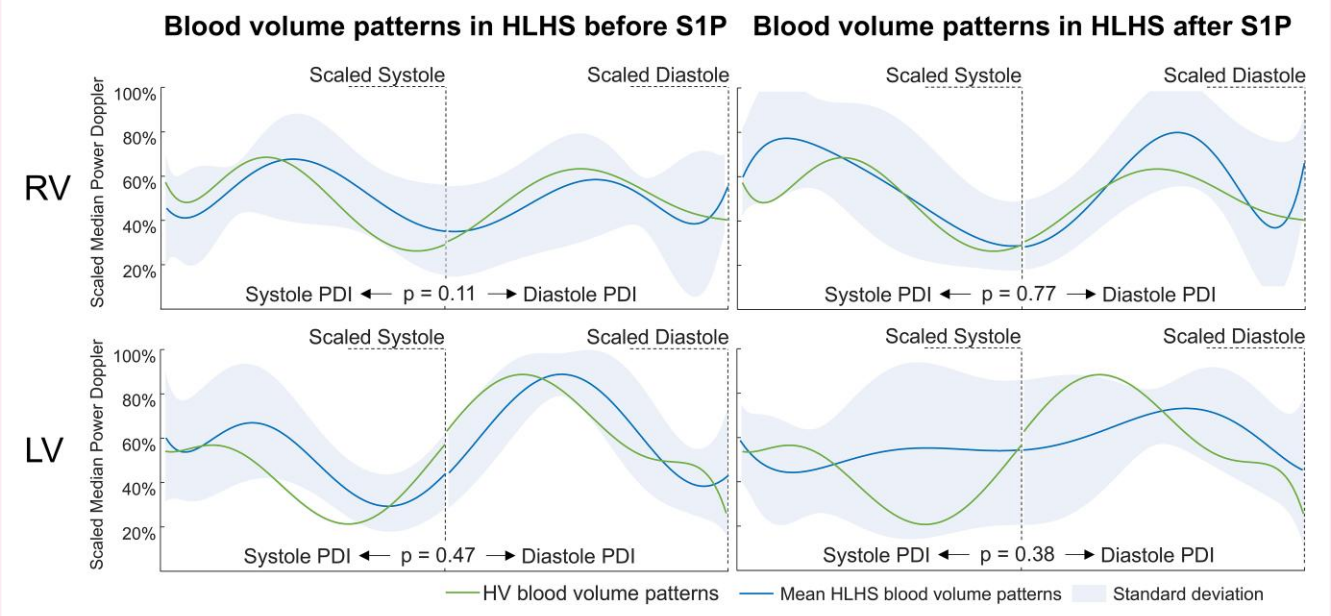

Figure 4 Temporal blood volume patterns in HLHS. The mean blood volume patterns of HLHS patients are presented. The blood volume patterns of HV are superimposed. *P*-value derived from *t*-test comparing the difference of percentage of the integral of the PD signals of systole compared with diastole.

assess patients' myocardial blood volumes over many days permitting a genuine prospective longitudinal cohort study to be performed. Finally, we included assessment of not only the left ventricle but the right ventricle as well, which provides additional clinical relevance to UPD assessments.

PD as a proxy for myocardial perfusion

In our study, myocardial blood volume patterns in healthy volunteers appear to correlate with epicardial coronary perfusion patterns. Myocardial perfusion is typically quantified as the volume of blood

moving through myocardial tissue per minute (mL/g/min).[8,21] PD techniques have been studied in conventional ultrasound to be highly sensitive to blood volume and proportional to hematocrit.[12,19] and are often used in clinical practice to resolve moving blood volumes (e.g. pulmonary venous drainage to the left atrium in foetal echocardiography).[22] Contrary to colour Doppler which is proportional to the local axial velocity of blood, PD is proportional to the local number of red blood cells. Therefore, it has the advantage over colour Doppler of being almost angle-independent and insensitive to aliasing effects. Using ultrasound contrast agents, Heinle *et al.*[23] already showed a strong correlation between PD and Tc-99m sestamibi single-photon emission computed tomography for coronary perfusion assessment in humans. Senior *et al.*[24] confirmed these data. In order to increase the sensitivity of the acoustic signal, the authors used a contrast agent (Sonovue; Bracco SpA, Milan, Italy), which can be avoided with UPD.[6,25] Even though we used linear imaging in our work without contrast agents, harmonic PD with ultrafast frame rates should be feasible. Correia *et al.*[17] already proposed ultrafast ultrasound sequences for harmonic imaging without contrast agents that could be readily applied to coronary perfusion imaging, potentially enhancing red blood cells backscattering and then improving blood detection. Moreover, this correlation between perfusion and blood volume assessed by PD has been explored and demonstrated in humans in multiple other organs such as the placenta, the brain, the kidneys, or the joints.[26–29] For coronary perfusion, the specific difficulty for conventional ultrasound has always been the large and rapid movements during the cycle which prevented sufficient sensitivity to quantify the signal variation. Ultrafast ultrasound imaging changes this paradigm and opens up a new avenue for ultrasound quantification.[10,11] Our work adds evidence to the link between the quantification of the amount of blood volume and the rate of moving blood volume: UPD blood volume patterns in both ventricles in healthy volunteers appear to coincide with patterns in perfusion rate seen in reference coronary perfusion studies in normal hearts (*Figure 2*). Therefore, we believe that assessing myocardial blood volume patterns using UPD adds clinically relevant information to the standard of care and could be complementary to conventional clinical measures of perfusion.

Potential mediators of changes in myocardial perfusion

Temporal fluctuations are influenced by myocardial-coronary flow distribution, transmural flow distribution, and myocardial vascular autoregulation.[8] In combination, this leads to an overall similar amount of perfusion (velocity of blood volume per gram of myocardial mass) in the RV and LV despite differences in coronary perfusion pressure.[8] In this study, we compared temporal changes at a local level, a myocardial segment which more directly assesses the coronary microvasculature, to myocardial perfusion patterns at a more global level, the epicardial coronary artery. While these are two different tools examining different levels, they should in theory measure a similar quantity assuming there are no abnormalities in coronary perfusion and autoregulation, a reasonable assumption in a healthy volunteer.[21] Indeed, on comparing our healthy volunteer perfusion patterns with reference values, we found them to be similar (*Figure 2*).

In congenital heart disease, many mediators of coronary blood perfusion could potentially be altered. For example, in TGA with a large patent ductus arteriosus, both ventricles are pressurized to the systemic vasculature: the right ventricle gives rise to the aorta, and the left ventricle is exposed to the patent ductus arteriosus. In our patients we see that both the RV and LV have a left ventricular reference pattern with a large peak in diastole and relatively flat in systole (*Figure 3*). However, after the ASO, the RV now is exclusively exposed to the pulmonary vasculature and the LV to the systemic vasculature with subsequent changes seen in the UPD perfusion tracings. These findings suggest that our data could be explained by changes in pressure of the ventricular cavity (chamber pressure). In a review paper, Goodwill *et al.*[8] describe the concept of a 'vascular waterfall' presented by Downey and Kirk in 1975, who stated that flow is dependent on the magnitude of the difference between arterial pressure and tissue pressure. Therefore, the pressure (systemic or sub-pulmonary) exerted on the myocardial tissue will have a direct impact on its perfusion and perfusion timing.[8] Additionally, the impact of myocardial contraction on myocardial perfusion includes recognition of variations in myocardial stiffness during the cardiac cycle (i.e. the varying elastance model). Knowing that myocardial stiffness varies during the cardiac cycle and is directly linked with the pressure generated by the chamber, it can be hypothesized that a higher-pressure cavity in systole will be less perfused than a lower-pressure cavity.[30] There are several other mediators to coronary perfusion that should impact our results. For example, the post-operative state may be influenced by vasoplegia within the coronary vasculature. However, our data were collected typically more than 7 days after the operation where a significant amount of autoregulation should likely be restored. Finally, there was no evidence of suboptimal coronary artery transfer (e.g. normal post-operative systolic function on clinical echocardiogram and typical recovery course) which reduces the likelihood that epicardial coronary stenosis impacted our findings.

In our HLHS cohort, we noted that there was no change in the RV or LV perfusion patterns after S1P. We could expect there to be no significant change with respect to coronary perfusion pressure since the RV continues to be the systemic ventricle. While there is a significant change in volume load, this may not be necessarily reflected in perfusion pattern changes within an intracardiac cycle. Surprisingly, the HLHS RV displays a perfusion pattern similar to a normal RV despite being pressurized by the systemic vasculature. There may be pathophysiologic explanations for this phenomenon at multiple levels. Firstly, the coronary microvasculature is well-documented to be pathologically altered in HLHS with significant fibrosis seen in foetal and neonatal specimens.[31–33] Additionally, angiographic studies of coronary perfusion is notable for a preference in blood flow during systole.[34] We speculate that our findings of abnormal temporal patterns in HLHS blood volumes potentially corroborate the evidence behind HLHS-related coronary microvascular dysfunction.

Clutter filtering of ultrafast ultrasound datasets

Blood and tissue signal separation, also known as clutter filtering, has experienced a significant evolution with ultrafast ultrasound compared with previous approaches. Traditional methods such as temporal high-pass filtering, linear regression, down-mixing of tissue velocity, and decorrelation algorithms were limited by the low number of temporal samples available for each spatial position due to the beam-scanning process of conventional ultrasound. The spatiotemporal continuity of samples provided by ultrafast ultrasound enables the differentiation of tissue and blood signals based on their distinct spatial and temporal coherence. Demené *et al.*[35] demonstrated that singular value decomposition could effectively separate tissue and blood signals into orthogonal subspaces, significantly improving the contrast-to-noise ratio as compared with previous methods, and revealing vessels with diameters as low as the ultrasound wavelength. This method was adapted to coronary imaging by Maresca *et al.*[10] and validated against a gold standard invasive flow probe.

Clinical implications

Assessing temporal patterns of myocardial blood volumes could be a useful adjunct tool with overall perfusion modalities [epicardial, coronary

blood flow, or cardiac magnetic resonance imaging (CMR), myocardial blood flow] to determine aetiologies of coronary artery-related cardiac dysfunction. To date, no non-invasive imaging technique allows quantification of temporal patterns of myocardial perfusion at the bedside, especially in children and neonates.[6] However, the evaluation of this parameter is important for the optimization of the management of certain patients. Post-ASO myocardial perfusion influences cardiac morbidity in TGA.[3,36,37] Effective myocardial perfusion is also thought to dictate adverse events in HLHS, especially the impact of diastolic runoff on early mortality when comparing modified Blalock-Taussig-Thomas to Sano shunts, but little research has been done to confirm these hypotheses.[5,38] Evaluating the degree of perfusion within the cardiac cycle, in addition to the overall perfusion rate, may help provide stronger prognostic tools to help guide decision-making.

Beyond the patient population explored in our study, quantitative assessment of myocardial perfusion is a major issue in congenital and acquired heart disease. In adults and in children, multiple other applications should be explored with this technique. Most clinical techniques assess this rate locally, either at a segment of the myocardium (e.g. myocardial blood perfusion via cardiac magnetic resonance imaging (CMR)] or at a more global level [e.g. epicardial coronary blood perfusion via cardiac conductance catheters), but these techniques are often expensive, time-consuming, and require contrast agents.[6,8] Being able to visualize the variation in coronary blood perfusion in a local myocardial segment has been infeasible due to limitations in spatial resolution (e.g. epicardial coronary conductance catheters unable to resolve individual myocardial segments) or temporal resolution (e.g. CMR techniques unable to resolve variations of blood flow within a cardiac cycle) of current diagnostic techniques. UPD could provide a portable, non-invasive, complement to understanding perfusion patterns in myocardial segments.

Limitations of our study

Currently, our approach is unable to directly compare absolute blood volumes between patients and events. Namely, while we can determine the relative degree of perfusion variation within a cardiac cycle, technical limitations prevent us from determining if there is relative ischaemia or hyperaemia between acquisitions. This is primarily due to PD's limitations, specifically ultrasound attenuation, which is impacted by the depth of ROI and tissue heterogeneity.[39] That said, tools, such as image registration to track gross myocardial motion, are actively being developed for UPD to facilitate the absolute quantification of myocardial blood volumes.[15,19]

A second technical limitation concerns our 2D approach. Maresca *et al.*[10] already explored this limitation related to out-of-plane motion. Quantification of the Doppler signal during a complete cardiac cycle using a static acoustic plane cannot incorporate myocardial movements, and thus the displacement of coronary vessels outside the explored plane is not accounted for. Performing UPD using a 3-dimensional approach with feature tracking of myocardial motion may circumvent this shortcoming.[27] Acquiring volumetric ultrafast ultrasound datasets usually requires cumbersome and expensive programmable scanners with enough electrical channels to drive an ultrasound probe with a transducer matrix array. However, recent developments in toroidal row-column-addressed probes may help to lift this technological barrier by enabling 3D ultrafast ultrasound imaging of the heart while keeping low electronic requirements.[40]

Our study is limited by sample size given the low incidence of CHD in the general population. The next step in this project is to perform a multicentre study which is challenging as few clinical centres have the technical capabilities to perform this study (e.g. develop novel acquisition sequences with an open programmable ultrasound system). We hope this study will motivate other teams to acquire this type of equipment to permit validation.

Lastly, while our imaging technique filters myocardial tissue from blood volume, acquiring an accurate assessment of hyperdynamic myocardial segments with a ROI deep to the probe continues to be challenging.[16] Namely, the small left ventricle and its anatomical position in HLHS patients lead to the selection of ROI only at the bottom of the images, which leads to a great standard deviation and a high risk of imprecise PD variation (*Figure 4*). Motion correction, such as image registration of the myocardium as mentioned previously, may help address this issue.

Conclusion

In this study, we quantitatively assessed myocardial blood volume variations using UPD and found them to be reflective of changes in haemodynamic and surgical status for neonates with congenital heart disease. This is the first step towards developing a portable and cost-effective method to quantify myocardial perfusion using transthoracic echocardiography. Future studies should focus on optimizing UPD to diagnose hyperaemia and ischaemia between patients, explore the correlation between blood volume variation and clinical outcomes, and validate the technique via a multicentre prospective study.

Supplementary data

Supplementary data are available at *European Heart Journal - Imaging Methods and Practice* online.

Acknowledgements

This study was supported by Canadian Institutes of Health Research (CIHR), 202203PJT-183888; Canada Foundation for Innovation (CFI) and the Ministry of Research and Innovation, Canada; Natural Sciences and Engineering Research Council of Canada (NSERC), Canada (RGPIN-2021-03539); the 2022 CCS-BMS HCM Research Award; and the Labatt Family Heart Centre at the Hospital for Sick Children, Toronto, Canada.

Conflict of interest: None declared.

Lead author biography

Dr. Nguyen is a Staff Pediatric Cardiologist and Assistant Professor in Pediatrics at Texas Children's Hospital who specializes in Pediatric Echocardiography. After his pediatric cardiology fellowship at Children's Hospital Los Angeles, he completed a research fellowship in echocardiography at the Hospital for Sick Children, University of Toronto, where he received training in clinical and translational research. His primary research interest is translating novel innovations in cardiac imaging to improve the care of children with acquired and congenital heart disease. His recent work involves applying machine learning to enhance the interpretation of conventional echocardiographic cardiac function assessment as well as developing novel ultrasound techniques to characterize the myocardium (e.g., non-invasive myocardial perfusion assessment and shear wave elastography). This research stands to benefit many children with heart disease including those with cardiomyopathies, Tetralogy of Fallot, and single ventricle palliation.

Dr. Zhang graduated from the Department of Medical Biophysics at the University of Toronto, specializing in the application of ultrafast ultrasound in pediatric cardiology. He focused on leveraging ultrafast ultrasound to quantify myocardial data, including myocardial blood volume and myocardial stiffness. His research aims to utilize ultrafast ultrasound as a diagnostic, monitoring, and screening tool for congenital heart disease. Dr. Zhang is CAMPEP-certified and is poised to exploring the synergy between ultrasound and radiotherapy, as well as other imaging technologies, to enhance therapeutic outcomes and reduce treatment cost.

Consent

Consent was obtained for all participants included in this study. For subjects under 18 years of age, assent was obtained when appropriate, and consent was provided by a parent or legal guardian. The study protocol was reviewed and approved by the appropriate institutional review board, ensuring compliance with ethical standards for human research.

Funding

This study was supported by Canadian Institutes of Health Research (CIHR), 202203PJT-183888; Canada Foundation for Innovation (CFI) and the Ministry of Research and Innovation, Canada; Thrasher Research Fund; and the Labatt Family Heart Centre at the Hospital for Sick Children, Toronto, Canada. All other authors have reported that they have no relationships relevant to the contents of this paper to disclose.

Data availability

The data underlying this article will be shared on reasonable request to the corresponding author.

Author contributions

Conceptualization: M.B., N.Z., J.B. O.V.; Data collection: M.B.; Data analysis: N.Z.; Data interpretation: M.B., N.Z., O.V.; Original draft preparation: N.F., N.Z., J.B., O.V.; Review and editing: M.B., N.Z., J.B., O.V., L.M., D.B., O.H., M.V.; M.B. and N.Z. contributed the same as co-first authors; O.V. and J.B. contributed the same as co-last authors. All authors approved the final version of the manuscript for publication.

References

1. Chen MY, Rochitte CE, Arbab-Zadeh A, Dewey M, George RT, Miller JM *et al.* Prognostic value of combined CT angiography and myocardial perfusion imaging versus invasive coronary angiography and nuclear stress perfusion imaging in the prediction of major adverse cardiovascular events: the CORE320 multicenter study. *Radiology* 2017; **284**:55–65.
2. Shekerdemian L. Perioperative manipulation of the circulation in children with congenital heart disease. *Heart* 2009;**95**:1286–96.
3. Nield LE, Dragulescu A, MacColl C, Manlhiot C, Brun H, McCrindle BW *et al.* Coronary artery Doppler patterns are associated with clinical outcomes post-arterial switch operation for transposition of the great arteries. *Eur Heart J Cardiovasc Imaging* 2018;**19**:461–8.
4. Sano S, Ishino K, Kawada M, Arai S, Kasahara S, Asai T *et al.* Right ventricle-pulmonary artery shunt in first-stage palliation of hypoplastic left heart syndrome. *J Thorac Cardiovasc Surg* 2003;**126**:504–9.
5. Ohye RG, Sleeper LA, Mahony L, Newburger JW, Pearson GD, Lu M *et al.* Comparison of shunt types in the Norwood procedure for single-ventricle lesions. *N Engl J Med* 2010;**362**:1980–92.
6. Villemain O, Baranger J, Jalal Z, Lam C, Calais J, Pernot M *et al.* Non-invasive imaging techniques to assess myocardial perfusion. *Expert Rev Med Devices* 2020.
7. Chatzizisis YS, Giannoglou GD, Parcharidis GE, Louridas GE. Is left coronary system more susceptible to atherosclerosis than right? A pathophysiological insight. *Int J Cardiol* 2007;**116**:7–13.
8. Goodwill AG, Dick GM, Kiel AM, Tune JD. Regulation of coronary blood flow HHS public access. *Compr Physiol* 2018;**7**:321–82.
9. Maresca D, Correia M, Tanter M, Ghaleb B, Pernot M. Adaptive spatiotemporal filtering for coronary ultrafast Doppler angiography. *IEEE Trans Ultrason Ferroelectr Freq Control* 2018;**65**:2201–4.
10. Maresca D, Correia M, Villemain O, Bizé A, Sambin L, Tanter M *et al.* Noninvasive imaging of the coronary vasculature using ultrafast ultrasound. *JACC Cardiovasc Imaging* 2018;**11**:798–808.
11. Villemain O, Baranger J, Friedberg MK, Papadacci C, Dizeux A, Messas E *et al.* Ultrafast ultrasound imaging in pediatric and adult cardiology: techniques, applications, and perspectives. *JACC Cardiovasc Imaging* 2020;**13**:1771–91.
12. Rubin JM, Bude RO, Carson PL, Bree RL, Adler RS. Power Doppler US: a potentially useful alternative to mean frequency- based color Doppler US. *Radiology* 1994;**190**:853–6.
13. Rubin JM, Bude RO, Fowlkes JB, Spratt RS, Carson PL, Adler RS. Normalizing fractional moving blood volume estimates with power Doppler US: defining a stable intravascular point with the cumulative power distribution function. *Radiology* 1997;**205**: 757–65.
14. Welsh AW, Rubin JM, Fowlkes JB, Fisk NM. Standardization of power Doppler quantification of blood flow in the human fetus using the aorta and inferior vena cava. *Ultrasound Obstet Gynecol* 2005;**26**:33–43.
15. Zhang N, Nguyen MB, Mertens L, Barron DJ, Villemain O, Baranger J. Improving coronary ultrafast Doppler angiography using fractional moving blood volume and motion-adaptive ensemble length. *Phys Med Biol* 2022;**67**:125021.
16. Baranger J, Mertens L, Villemain O. Blood flow imaging with ultrafast Doppler. *J Vis Exp* 2020;**14**:164.
17. Correia M, Provost J, Chatelin S, Villemain O, Tanter M, Pernot M. Ultrafast harmonic coherent compound (UHCC) imaging for high frame rate echocardiography and shear-wave elastography. *IEEE Trans Ultrason Ferroelectr Freq Control* 2016;**63**:420–31.
18. Lopez L, Saurers DL, Barker PCA, Cohen MS, Colan SD, Dwyer J *et al.* Guidelines for performing a comprehensive pediatric transthoracic echocardiogram: recommendations from the American society of echocardiography. *J Am Soc Echocardiogr* 2024;**37**: 119–70.
19. Rubin JM, Adler RS, Fowlkes JB, Spratt S, Pallister JE, Chen JF *et al.* Fractional moving blood volume: estimation with power Doppler US. *Radiology* 1995;**197**:183–90.
20. Nguyen MB, Zhang N, Aguet J, Venet M, Fan CPS, Mertens LL *et al.* Towards transthoracic quantitative myocardial perfusion assessment using ultrafast ultrasound imaging. *J Am Coll Cardiol* 2023;**81**(8_Supplement):1531.
21. Camici PG, D'Amati G, Rimoldi O. Coronary microvascular dysfunction: mechanisms and functional assessment. *Nat Rev Cardiol* 2015;**12**:48–62.
22. Moon-Grady AJ, Donofrio MT, Gelehrter S, Hornberger L, Kreeger J, Lee W *et al.* Guidelines and recommendations for performance of the fetal echocardiogram: an update from the American society of echocardiography. *J Am Soc Echocardiogr* 2023;**36**: 679–723.
23. Heinle SK, Noblin J, Goree-Best P, Mello A, Ravad G, Mull S *et al.* Assessment of myocardial perfusion by harmonic power Doppler imaging at rest and during adenosine stress: comparison with 99mTc-sestamibi SPECT imaging. *Circulation* 2000;**102**: 55–60.
24. Senior R, Kaul S, Soman P, Lahiri A. Power Doppler harmonic imaging: a feasibility study of a new technique for the assessment of myocardial perfusion. *Am Heart J* 2000; **139**(2 Pt 1):245–51.
25. Venet M, Friedberg MK, Mertens L, Baranger J, Jalal Z, Tlili G *et al.* Nuclear imaging in pediatric cardiology: principles and applications. *Front Pediatr* 2022;**10**:909994.
26. Guiot C, Gaglioti P, Oberto M, Piccoli E, Rosato R, Todros T. Is three-dimensional power Doppler ultrasound useful in the assessment of placental perfusion in normal and growth-restricted pregnancies? *Ultrasound Obstet Gynecol* 2008;**31**:171–6.
27. Correas JM, Anglicheau D, Joly D, Gennisson JL, Tanter M, Hélénon O. Ultrasound-based imaging methods of the kidney—recent developments. *Kidney Int* 2016;**90**:1199–210.
28. Filippucci E, Iagnocco A, Salaffi F, Cerioni A, Valesini G, Grassi W. Power Doppler sonography monitoring of synovial perfusion at the wrist joints in patients with rheumatoid arthritis treated with Adalimumab. *Ann Rheum Dis* 2006;**65**:1433–7.
29. Zeng S, Zhou J, Peng Q, Tian L, Xu G, Zhao Y *et al.* Assessment by three-dimensional power Doppler ultrasound of cerebral blood flow perfusion in fetuses with congenital heart disease. *Ultrasound Obstet Gynecol* 2015;**45**:649–56.
30. Pernot M, Couade M, Mateo P, Crozatier B, Fischmeister R, Tanter M. Real-time assessment of myocardial contractility using shear wave imaging. *J Am Coll Cardiol* 2011;**58**: 65–72.
31. O'Connor WN, Cash JB, Cottrill CM, Johnson GL, Noonan JA. Ventriculocoronary connections in hypoplastic left hearts: an autopsy microscopic study. *Circulation* 1982; **66**:1078–86.

32. Salih C, Sheppard MN, Ho SY. Morphometry of coronary capillaries in hypoplastic left heart syndrome. *Ann Thorac Surg* 2004;**77**:903–7.
33. Cole CR, Eghtesady P. The myocardial and coronary histopathology and pathogenesis of hypoplastic left heart syndrome. *Cardiol Young* 2016;**26**:19–29.
34. Freedom RM, Culham JA, Moes CA, Harrington DP. Selective aortic root angiography in the hypoplastic left heart syndrome. *Eur J Cardiol* 1976;**4**:25–9.
35. Demené C, Deffieux T, Pernot M, Osmanski BF, Biran V, Gennisson JL *et al.* Spatiotemporal clutter filtering of ultrafast ultrasound data highly increases Doppler and ultrasound sensitivity. *IEEE Trans Med Imaging* 2015;**34**:2271–85.
36. Villafañe J, Lantin-Hermoso MR, Bhatt AB, Tweddell JS, Geva T, Nathan M *et al.* D-transposition of the great arteries: the current era of the arterial switch operation. *J Am Coll Cardiol* 2014;**64**:498–511.
37. Anderson BR, Ciarleglio AJ, Hayes DA, Quaegebeur JM, Vincent JA, Bacha EA. Earlier arterial switch operation improves outcomes and reduces costs for neonates with transposition of the great arteries. *J Am Coll Cardiol* 2014;**63**:481–7.
38. Rickers C, Wegner P, Silberbach M, Madriago E, Gabbert DD, Kheradvar A *et al.* Myocardial perfusion in hypoplastic left heart syndrome. *Circ Cardiovasc Imaging* 2021; **14**:e012468.
39. Hernandez-Andrade E, Jansson T, Ley D, Bellander M, Persson M, Lingman G *et al.* Validation of fractional moving blood volume measurement with power Doppler ultrasound in an experimental sheep model. *Ultrasound Obstet Gynecol* 2004;**23**:363–8.
40. Caudoux M, Demeulenaere O, Porée J, Sauvage J, Mateo P, Ghaleb B *et al.* Curved toroidal row column addressed transducer for 3D ultrafast ultrasound imaging. *IEEE Trans Med Imaging* 2024;**43**:3279–91.